International Journal of Power Electronics and Drive System (IJPEDS)
Vol. 17, No. 1, March 2026, pp. 11~24
ISSN: 2088-8694, DOI: 10.11591/ijpeds.v17.i1.pp11-24

Design of the wireless EV charger to meet the performance requirement of SAE J2954 standard

Patcharapon Kaewnoen, Supapong Nutwong, Nattapong Hatchavanich, Ekkachai Mujjalinvimut
Department of Electrical Engineering, King Mongkut's University of Technology Thonburi, Bangkok, Thailand

Article Info

Article history:

Received Jul 5, 2025
Revised Oct 24, 2025
Accepted Dec 11, 2025

Keywords:

Circular flat spiral coil
Coil design
Performance requirement
SAE J2954 standard
Wireless EV charger

ABSTRACT

To address the need for a reproducible design process for an efficient wireless electric vehicle (EV) charging system that guarantees compliance with the SAE J2954 standard, this paper proposes a systematic, flowchart-based optimization technique. Unlike methods that focus solely on coil performance, the proposed approach integrates standard-specific constraints, such as inductance and geometric limits, from the outset to ensure the final design meets stringent performance benchmarks for efficiency and misalignment tolerance. A circular flat spiral coil structure has been adopted for both the transmitter and receiver coils to enhance manufacturability and achieve uniform magnetic field distribution. A flowchart-based design technique has been developed to optimize key coil parameters, including the number of turns and coil diameters, subject to constraints of 200 µH inductance and a maximum outer diameter of 700 mm. Finite element analysis (FEA) simulations verify that the proposed design approach achieves maximum magnetic coupling under various air gap distances and misalignment conditions. An experimental validation of a 2-kW prototype demonstrates close agreement with simulations, achieving coil-to-coil efficiencies between 92.61% and 96.67%, and overall system efficiency exceeds 80% under all tested conditions. These results confirm that the proposed design method effectively meets performance requirements set by the SAE J2954 standard.

Corresponding Author:

Supapong Nutwong
Department of Electrical Engineering, King Mongkut's University of Technology Thonburi
126 Pracha Uthit Rd., Bang Mod, Thung Khru, Bangkok 10140, Thailand
Email: supapong.nut@kmutt.ac.th

1. INTRODUCTION

Electric vehicles (EVs) are becoming a major part of the automotive industry, driven by increasing demand and a shift toward more sustainable transportation. According to the International Energy Agency (IEA), global EV sales surpassed 14 million units in 2023, and this number is expected to grow even more in the coming years [1]. One of the main reasons behind this growth is that EVs offer lower fuel and maintenance costs compared to traditional gasoline-powered vehicles [2].

Conventional plug-in charging systems for EVs have some significant drawbacks in terms of usability and safety. Connecting and handling heavy charging cables can be inconvenient, especially in bad weather conditions. Over time, frequent use can wear out charging ports and connectors, leading to higher maintenance costs and an increased risk of system failures. In wet conditions, moisture can damage cable insulation and connectors, increasing the risk of short circuits and leakage currents, which can cause electric shocks or even fires. Leakage currents are one of the leading causes of charging-related electrical failures, where multiple reports linking them to system malfunctions [3]-[5].

Wireless power transfer (WPT) technology has emerged as a more convenient and safer alternative by eliminating physical connectors. This substantially reduces the risks of electric shock, leakage currents, and other electrical failures commonly associated with traditional plug-in systems [6]-[8]. Wireless chargers for EVs have developed significantly over the past decade. This technology enables power transmission through magnetic coupling between the ground assembly (GA) and vehicle assembly (VA) without requiring any physical contact. Recent developments have shown that optimized WPT systems can achieve power transfer efficiencies exceeding 80% under various operating conditions [9]-[12]. However, implementing wireless charging systems faces several technical challenges, including efficiency optimization, electromagnetic compatibility (EMC), and safety considerations [13]-[17].

To ensure reliable and standardized wireless charging solutions for EVs, the Society of Automotive Engineers (SAE) has established the J2954 standard [18] for light-duty electric vehicles. This standard introduces crucial guidelines for categorizing the wireless EVs charging system, including input power (WPT power classes), vertical distance between transmitting and receiving coils (WPT Z-Classes), ground assembly installation categories, and interoperability classifications. Additionally, it specifies the requirements of output voltage, output power, maximum allowable coil misalignment, operating frequency, input power factor, and minimum system efficiency in both with and without coil misalignment.

The design and development of wireless EV charging systems in accordance with the SAE J2954 standard have been explored extensively in prior research. In response to the rising power requirements of wireless EV chargers, a study in [19] introduces a modular multilevel converter (MMC). An integrated boost multilevel converter (IBMC) with a primary-side control technique is proposed in [20], which achieves a boosted multilevel output voltage while eliminating additional components on the receiver side. To achieve a high coupling coefficient, increased tolerance to misalignment, and enhanced power efficiency, [21] proposes a double set square (DSSq) charging pad design for the receiver coil. In systems without parking assistance, a split flat solenoid coupler is proposed in [22] to increase lateral misalignment tolerance while reducing copper and ferrite material usage. A receiver coil with a dual-layer structure and an M-core is introduced in [23], which enhances the power density and coupling coefficient of the receiver.

However, there is a lack of comprehensive design approaches for developing wireless EV charging systems that fully comply with the SAE J2954 standard, particularly regarding the optimization of coil design to achieve the most suitable structure for maximizing power transfer efficiency and improving misalignment tolerance. This paper aims to develop an optimal design approach for efficient wireless EV chargers that meet the performance requirements of the SAE J2954 standard, with a focus on the design of the transmitter and receiver coils. The design methodology is presented and subsequently verified through magnetic simulations using the COMSOL program. Finally, experimental validation is performed on a 2-kW wireless EV charging system.

2. SAE J2954 STANDARD OVERVIEW

The SAE J2954 standard establishes globally recognized guidelines and requirements for wireless charging systems, specifically tailored for light-duty electric vehicles. It defines acceptable criteria for interoperability, electromagnetic compatibility (EMC), EMF exposure, minimum performance, safety, and testing for WPT of electric vehicles. The WPT system described in this standard consists of two main parts: the ground assembly (GA) and the vehicle assembly (VA), as shown in Figure 1. The electrical energy provided by the utility grid is first converted into DC and subsequently into high-frequency alternating current (AC) through GA electronics. It is then wirelessly transmitted to the VA via electromagnetic coupling between the GA and VA coils. Before delivering the received power to the EV's battery, the induced high-frequency AC is rectified by the VA electronics.

This standard classifies wireless EV charging systems based on the maximum input apparent power drawn from the grid (WPT power classes), the range of ground clearances (WPT Z-classes), ground assembly installation types, and interoperability. The three WPT power classes are WPT1 (3.7 kVA), WPT2 (7.7 kVA), and WPT3 (11.1 kVA). The WPT Z-classed are defined based on the vertical clearance between the ground and the lower surface of the VA coil, known as the VA coil ground clearance. The WPT Z-classes include Z1 (100–150 mm), Z2 (140–210 mm), and Z3 (170–250 mm). This standard defines three GA installation categories based on their mounting position relative to the ground surface, which are above-ground mounting (GA is placed on top of the ground surface), flush mounting (GA is installed flush with the ground surface), and buried mounting (GA is buried below the ground surface). To ensure compatibility with VA, this standard defines two interoperability classifications for GA. Interoperability Class I GA refers to a GA that is intended for public use (multiple VA), capable of operating across the full range of VA coil ground clearances and input power range. Interoperability Class II GA refers to a GA that is intended for a specific use (specific VA). It may operate over less than the full VA coil ground clearance range and input

power range. According to this standard, the designed system in this work is classified as detailed in Table 1. To ensure the reliable and efficient operation of wireless EV charging systems, performance requirements have been established by the SAE J2954 standard. Based on this standard and the system classification shown in Table 1, the minimum performance requirements for the designed WPT system are specified in Table 2.

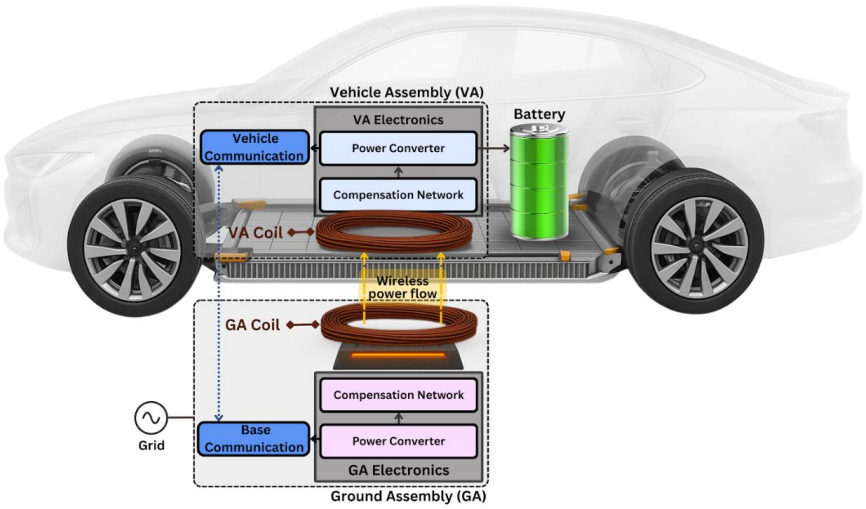

Figure 1. Overall WPT system as defined in the SAE J2954 standard

Table 1. Classification of the WPT system under design according to SAE J2954 standard

SAE J2954 classification	Designing system	Description
WPT power class	WPT1	Maximum input apparent power: 3.7 kVA
WPT Z-Classes	Z1	VA coil ground clearance: 100 – 150 mm
Ground assembly installation	Above ground mounting	GA installation: Above ground
Interoperability	Class II GA	GA compatible with specific VA units

Table 2. Required performance of the WPT system under design according to SAE J2954 standard

Parameters	Value
Rated output power	2 kW
Input apparent power at rated output power	≤ 3.7 kVA
Output DC voltage at rated output power	280 – 420 V
System efficiency at rated output power (Air gap = 10 cm, No Misalignment)	≥ 85%
System efficiency at rated output power (Air gap = 10 cm, Misalignment = 10 cm)	≥ 80%
System efficiency at rated output power (Air gap = 15 cm, No Misalignment)	≥ 85%
System efficiency at rated output power (Air gap = 15 cm, Misalignment = 10 cm)	≥ 80%
Frequency	85 kHz

3. SYSTEM DESCRIPTION AND ANALYSIS

The wireless EV charging system illustrated in Figure 1 can be represented by the equivalent circuit depicted in Figure 2(a), where V_{in} represents the first harmonic component of an inverter output voltage. The inductance of the transmitter (GA) coil, receiver (VA) coil, and mutual inductance are denoted by L_p, L_s, and M, respectively. The intrinsic resistances of the GA coil and VA coil are defined as R_p and R_s. The series-series (SS) compensation topology is adopted by connecting a capacitor with capacitance C_p in series with the GA coil and a capacitor with capacitance C_s in series with the VA coil. Both the transmitter and receiver circuits are tuned to resonate at the same frequency, defined as the resonant frequency (f_0).

The system output can be represented by an equivalent AC resistance (R_{ac}), calculated as (1) [24].

$$R_{ac} = \frac{8R_{dc}}{\pi^2} \quad (1)$$

Where R_{dc} is the equivalent DC resistance, determined by the voltage and current ratings of the EV battery. To ensure the system operates at a resonant frequency, the required capacitance values for the transmitter and receiver circuits are as (2) and (3).

$$C_p = \frac{1}{4\pi^2 f_0^2 L_p} \quad (2)$$

$$C_s = \frac{1}{4\pi^2 f_0^2 L_s} \quad (3)$$

By transferring the impedance in the receiver circuit to the transmitter circuit, the system can be simplified as shown in Figure 2(b), where Z_r is defined as the reflected impedance, which is expressed as (4).

$$\vec{Z}_r = \frac{4L_p L_s \pi^2 f_0^2 k^2}{R_s + R_{ac}} \quad (4)$$

Where $k = M/\sqrt{L_p L_s}$ is the magnetic coupling coefficient of a coupled coil. The coil-to-coil efficiency (η_{coil}) can be derived from (5), which depends heavily on the magnetic coupling coefficient (k); that is, η_{coil} increases as k increases. It is noted that a well-designed coil can maximize the coupling factor.

$$\eta_{coil} = \frac{4R_{ac} L_p L_s \pi^2 f_0^2 k^2}{(R_p + \vec{Z}_r)(R_s + R_{ac})^2} \quad (5)$$

Commonly used structures of coupled coils for wireless EV charging systems are the circular flat spiral coil (CFSC), square flat spiral coil (SFSC), double D pad (DD), double D-quadrature pad (DDQ), and bi-polar pad (BP). A comparison of these structures is reported in [25], which can be summarized in Table 3. It is noted that the CFSC structure requires low space volume and material usage, thereby lowering the overall system cost. Moreover, it provides a uniform magnetic field distribution, scalability, and manufacturability [26].

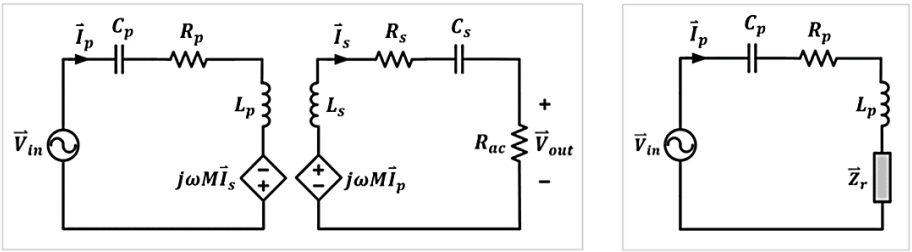

(a) (b)

Figure 2. Equivalent circuit of the wireless EV charging system: (a) full circuit and (b) simplified circuit

Table 3. Comparison of the coupled coils structures used in a wireless EV charger

Structure	Misalignment tolerance	Space volume	Material usage
CFSC	Weak	Low	Low
SFSC	Weak	Low	Low
DD	Medium	Medium	Medium
DDQ	Medium	Medium	High
BP	Preferable	Medium	Medium

4. PROPOSED DESIGN TECHNIQUE

To meet the performance requirements of the SAE J2954 standard, as detailed in Table 2, this work focuses on the optimal design of a coupled coil for the wireless charging system. A circular flat spiral coil configuration, as shown in Figure 3, is adopted due to its key advantages, including ease of design, manufacturability, and uniform magnetic field distribution. The coil's inner diameter, coil's outer diameter, copper wire's cross-sectional area, and spacing between coil turns are represented by d_i, d_o, w, and s, respectively.

Various research efforts have proposed design methodologies to optimize the parameters of circular flat spiral coils; nevertheless, most of these studies emphasize system performance without referencing or conforming to established international standards. In this work, a systematic, flowchart-based optimization technique is proposed to provide a reproducible design process for an efficient wireless electric vehicle (EV) charging system that ensures compliance with the SAE J2954 standard. A comparison between the previously optimized design technique and the proposed design approach is presented in Table 4.

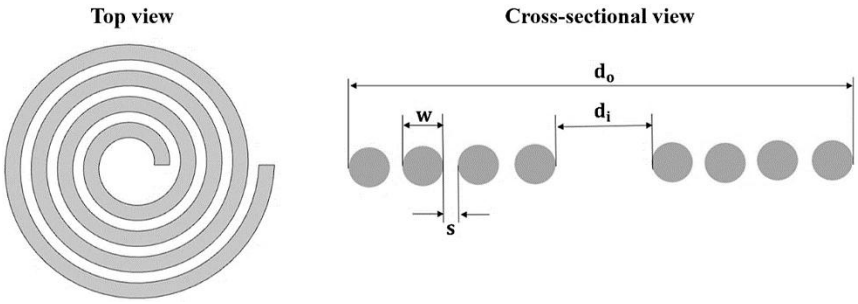

Figure 3. Circular flat spiral coil configuration

Table 4. Comparison between the previously optimized design technique and the proposed method

Sources	Optimized design technique	SAE J2954 compliance
[27]	Coil size ratio-based	×
[28]	Model-based	×
[29]	Machine learning	×
[30]	Genetic algorithm	×
[31]	Genetic algorithm	×
[32]	Flowchart-based	×
This work	Flowchart-based	✓

As presented in [30], in the case of zero turn spacing (s = 0), the self-inductance of a circular flat spiral coil (in μH) can be estimated as (6).

$$L = \frac{(d_i+wN)^2N^2}{406.4d_i+1524wN} \quad (6)$$

Where N is the number of turns of the coil. Note that d_i, d_o, and w are measured in millimeters. The estimated coil inductance will be within 5% of the actual value if the condition in (7) is met. This condition is called the Wheeler Condition, or WC for short.

$$0.9wN - 0.1d_i > 0 \quad (7)$$

From (6), the coil inner diameter can be derived as presented in (8), while the coil outer diameter can be computed from (9).

$$d_i = \frac{0.2\left(1016L+2\sqrt{258064L^2+6985wLN^3}-5wN^3\right)}{N^2} \quad (8)$$

$$d_o = di + 2wN \quad (9)$$

To achieve an optimal coupled coil that provides the maximum magnetic coupling coefficient, this work proposes a design technique, shown as the flowchart in Figure 4. It is assumed that the transmitter and receiver coils are identical. With this technique, the optimal coil turn number (N), coil inner diameter (d_i), and coil outer diameter (d_o) are obtained through an iterative calculation process. The design constraints, including coil inductance (L), turn spacing (s), copper wire diameter (w), and maximum coil outer diameter ($d_{o,max}$), are defined in the first step. Next, the calculation loop begins by setting the initial coil turn number to one. The coil inner diameter is then calculated using (8). After that, the coil outer diameter is calculated using (9). Then, it is compared with $d_{o,max}$. If it is greater than $d_{o,max}$, meaning the outer diameter of the coil exceeds the constraint, the current value of N cannot be used. Thus, the coil turn number will be updated by increasing its previous value by one, and the process will return to the d_i calculation stage. But if it is lower than $d_{o,max}$, the process will continue to check the Wheeler condition (WC) in (7) to ensure that the difference between the estimated and actual coil inductance values is less than 5%. If this condition is not met, the coil turn number will also be updated, as explained earlier. But if this condition is met, the latest value of N, d_i, and d_o will be assigned as the optimal value, and the design process will stop. Using the proposed technique, applied under the design constraints in Table 5, yields the optimal parameters for the coupled coil of the wireless EV charger, as shown in Table 6.

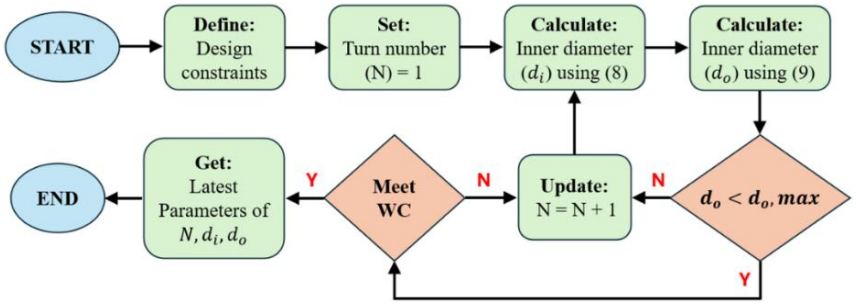

Figure 4. Proposed optimal coil design flowchart

Table 5. Constraints for the coil design

Parameter	Value
Coil inductance (L)	200 µH
Turn spacing (s)	0 mm
Copper wire diameter (w)	4 mm
Maximum coil outer diameter ($d_{o,max}$)	700 mm

Table 6. Optimal coil design results

N (turns)	d_i (mm)	d_o (mm)	WC	Remark
1	81,286.99	81,294.99	Fail	$d_o > d_{o,max}$
2	20,334.44	20,349.97	Fail	$d_o > d_{o,max}$
3	9,051.99	9,075.99	Fail	$d_o > d_{o,max}$
4	5,107.63	5,139.63	Fail	$d_o > d_{o,max}$
5	3,285.30	3,325.30	Fail	$d_o > d_{o,max}$
6	2,297.95	2,345.95	Fail	$d_o > d_{o,max}$
7	1,704.50	1,760.50	Fail	$d_o > d_{o,max}$
8	1,320.62	1,384.62	Fail	$d_o > d_{o,max}$
9	1,058.24	1,130.24	Fail	$d_o > d_{o,max}$
10	870.95	950.948	Fail	$d_o > d_{o,max}$
11	732.42	820.42	Fail	$d_o > d_{o,max}$
12	626.85	722.85	Fail	$d_o > d_{o,max}$
13	544.29	648.29	Fail	WC not met
14	478.23	590.23	Pass	Optimal value
15	424.32	544.32	Pass	Sufficient value
16	379.50	507.50	Pass	Sufficient value
17	341.64	477.64	Pass	Sufficient value
18	309.17	453.17	Pass	Sufficient value
19	280.97	432.97	Pass	Sufficient value
20	256.18	416.18	Pass	Sufficient value

As indicated in Table 6, the optimal coil parameters are achieved at iteration $N = 14$. At this stage, the coil's inner and outer diameters are 478.23 mm and 590.23 mm, respectively. Note that the outer diameter is within the maximum limit of 700 mm, and the design meets the wheeler condition. For comparison, further iterations from $N = 15$ to $N = 20$ were conducted. The results show that the wheeler condition is met and $d_o < d_{o,max}$ at these stages. However, they do not yield the optimal coil parameters, which are defined as the sufficient value.

To verify the presented coil design results, a finite element analysis (FEA) simulation was performed using COMSOL multiphysics software, as shown in Figure 5. The coil parameters listed in Table 5 (s and w) and those for iterations N = 14 to 20 in Table 6 (N, d_i, and d_o) were used in the simulation. The coil alignment conditions, as specified by the performance requirements in Table 2, were simulated. These conditions include a 10 cm air gap both with and without a 10 cm horizontal misalignment, and a 15 cm air gap both with and without a 10 cm horizontal misalignment.

The FEA simulation results presented in Figure 6 indicate that the highest magnetic coupling coefficient of the coupled coil, under all coil alignment conditions, occurs when the coil turn number is 14, which corresponds to the optimal value obtained from the coil design. The magnetic coupling decreases as the coil turn number increases, which verifies the proposed design method. Moreover, for a given coil turn number, the results indicate that magnetic coupling decreases with increasing air gap and/or horizontal misalignment between the coils.

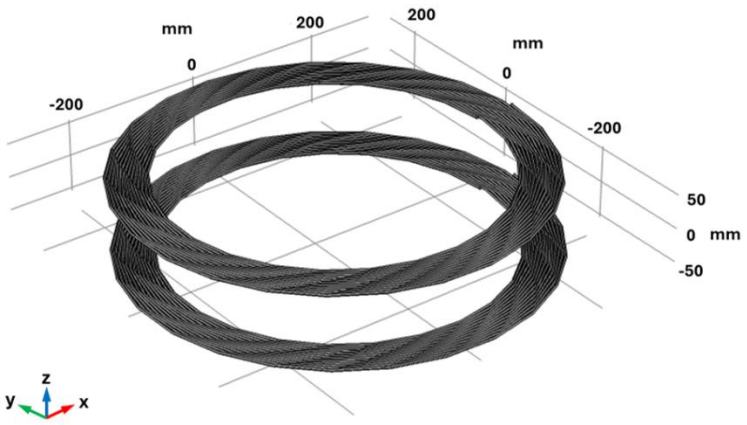

Figure 5. COMSOL multiphysics FEA simulation

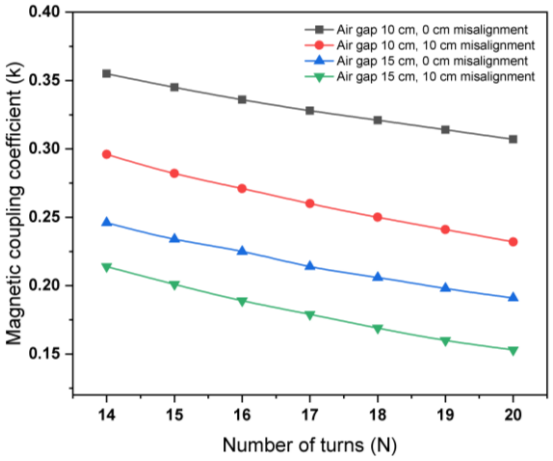

Figure 6. FEA simulation results

5. EXPERIMENTAL RESULTS AND DISCUSSION

To validate the proposed technique, the transmitter (Tx) and receiver (Rx) coils are fabricated, as illustrated in Figure 7, using the optimal coil parameters derived from the design process, which are N = 14 turns, s = 0 mm, w = 4 mm, d_i = 478.23 mm, and d_o = 590.23 mm. The inductance measured for the Tx coil is 200.89 μH and the Rx coil is 204.78 μH, which deviates from the designed value of 200 μH by 0.445% and 2.39%, respectively. These errors are within 5%, confirming the validity of the wheeler condition.

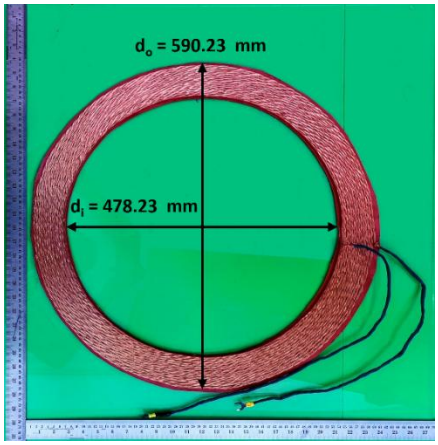

Figure 7. Fabricated coil designed with the optimal coil parameters

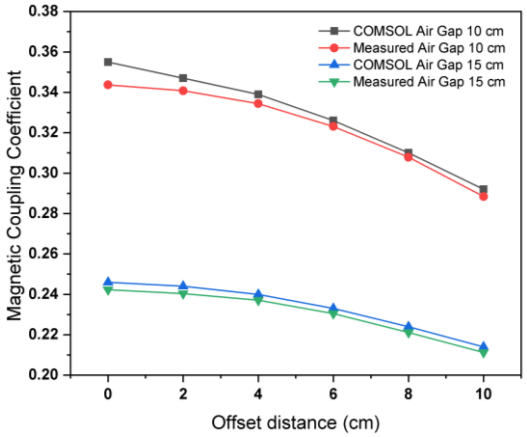

Figure 8. Results of the magnetic coupling coefficient at different offset distances

The magnetic coupling coefficient of the coupled coils was measured as a function of horizontal misalignment (offset distance) from 0 cm to 10 cm, and the results are shown in Figure 8. Two air gaps (vertical distances) between the coils are considered, which are 10 cm and 15 cm. The results are in close agreement with those presented in Figure 6, which show that magnetic coupling decreases with increasing air gap and/or horizontal misalignment between the coils. Furthermore, the errors between the measured and FEA simulation results are less than 3%.

The experimental validation was performed on a 2-kW prototype, as depicted in Figure 9, with its equivalent circuit illustrated in Figure 10. The components on the transmitter side include a variable three-phase voltage source (3-phase variac), a three-phase full-wave rectifier (input rectifier), a full-bridge inverter, a transmitter coil (Tx coil), and a compensation capacitor (C_p). On the receiver side, the system consists of a receiver coil (Rx coil), a compensation capacitor (C_s), a single-phase full-wave rectifier (output rectifier), and a load resistor. The circuit parameters were measured and are listed in Table 7.

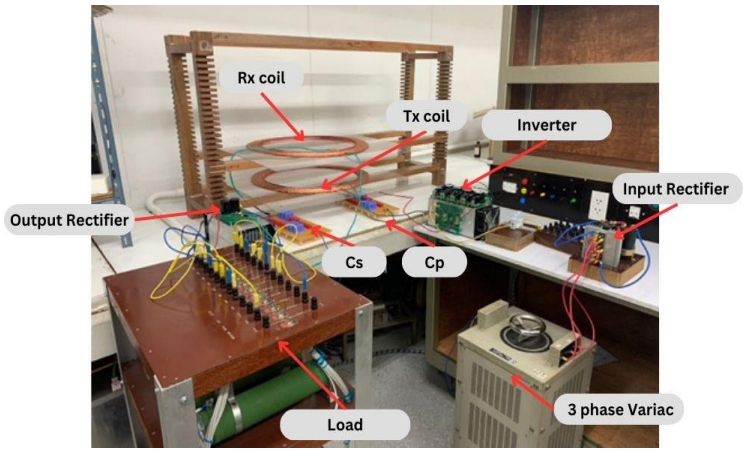

Figure 9. A 2-kW prototype of a wireless EV charging system

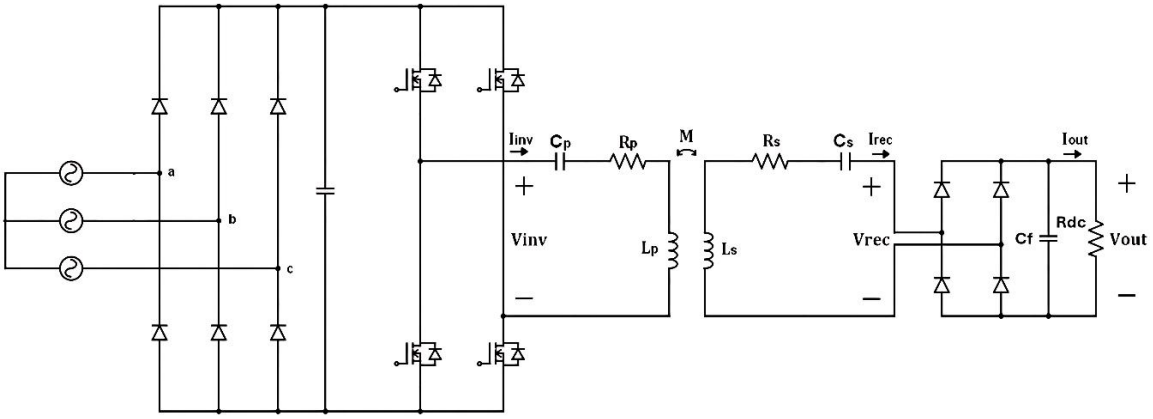

Figure 10. Equivalent circuit of the experimental setup

Table 7. Measured parameters of the wireless EV charging system prototype

Parameters	Value
Self-inductance of Tx coil (L_p)	200.89 µH
Self-inductance of Rx coil (L_s)	204.78 µH
Mutual inductance (M) at air gap = 10 cm, horizontal misalignment = 0 cm	69.7 µH
Mutual inductance (M) at air gap = 10 cm, horizontal misalignment = 10 cm	58.5 µH
Mutual inductance (M) at air gap = 15 cm, horizontal misalignment = 0 cm	48.9 µH
Mutual inductance (M) at air gap = 15 cm, horizontal misalignment = 10 cm	42.6 µH
Compensation capacitor at transmitter side (C_p)	17.394 nF
Compensation capacitor at receiver side (C_s)	17.411 nF
Intrinsic resistance of Tx coil (R_p)	0.385 Ω
Intrinsic resistance of Rx coil (R_s)	0.392 Ω
Load resistance (R_{dc})	48 Ω

The measured system efficiency for the 10 cm and 15 cm air gap cases is shown in Figure 11 under different horizontal misalignment conditions ranging from 0 to 10 cm. Note that the system efficiency is calculated as the ratio of the DC output power to the input AC power ($\eta_{sys} = P_{out,dc}/P_{in,ac}$). In all cases, the output power is kept constant at approximately 2 kW by adjusting the input AC voltage using a variable three-phase source (three-phase variac). It shows that system efficiency decreases as the air gap and/or horizontal misalignment increases, which aligns with the results in Figure 8. The system efficiencies exceed 85% and 80% for the 0 cm and 10 cm horizontal misalignment cases, respectively.

Figure 12 presents the experimental waveforms for the 10 cm air gap case, where P_{inv} is the product of inverter voltage (V_{inv}) and inverter current (I_{inv}), and P_{rec} is the product of rectifier voltage (V_{rec}) and rectifier current (I_{rec}). The coil-to-coil efficiency (η_{coil}) can be calculated by dividing the average value of P_{rec} by the average value of P_{inv}. For the cases of 0 cm and 10 cm horizontal misalignment, the η_{coil} are 96.67% and 95.19%, respectively.

Figure 13 presents the experimental waveforms for the larger 15 cm air gap condition, which represents a more challenging scenario for power transfer. As shown, the coil-to-coil efficiency was measured at 94.52% with perfect alignment and 92.61% with a 10 cm horizontal offset. When compared to the 10 cm air gap results in Figure 12, these values represent a drop in efficiency of approximately 2-3%, which directly corresponds to the weaker magnetic coupling coefficient (k) at greater distances, as predicted by the FEA simulations in Figure 6. Despite this reduction, the efficiencies remain high, validating that the optimized coil design is robust even under less-than-ideal vertical and horizontal positioning.

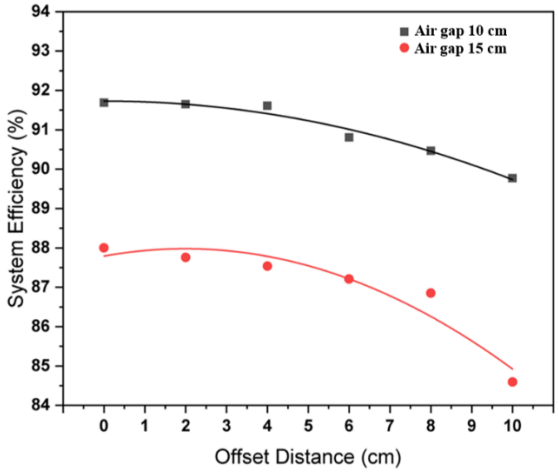

Figure 11. Measured system efficiency values at different horizontal misalignments (offset distance)

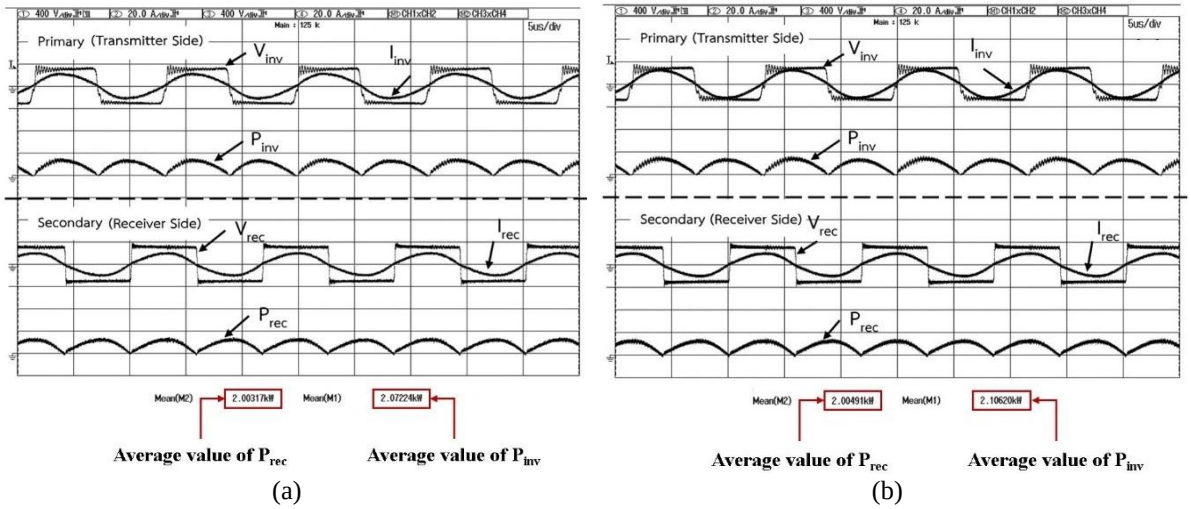

Figure 12. Experimental waveforms at 10 cm air gap: (a) 0 cm horizontal misalignment and (b) 10 cm horizontal misalignment

To evaluate the system prototype, the test results are compared with the performance requirements of SAE J2954, as specified in Table 2. The evaluation results presented in Table 8 indicate that the designed system meets all the requirements. This result confirms the validity of the proposed design methodology.

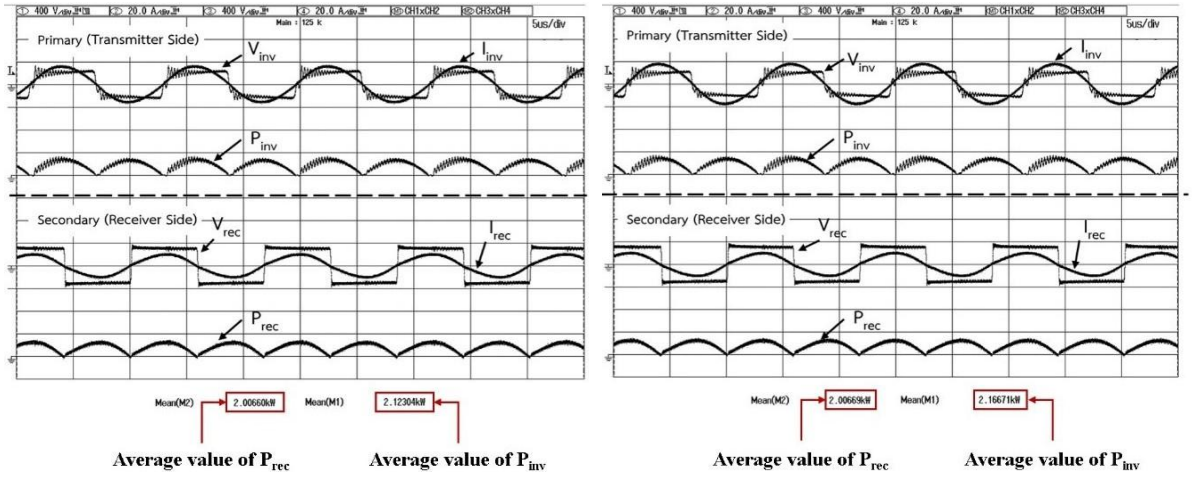

Figure 13. Experimental waveforms at 15 cm air gap: (a) 0 cm horizontal misalignment and (b) 10 cm horizontal misalignment

Table 8. Evaluation of system performance against SAE J2954 standard

Performance parameters	SAE J2954 requirement	Measured results	Evaluation
Input apparent power at rated output of 2 kW	≤ 3.7 kVA	2.28 - 2.6 kVA	Pass
DC output voltage at rated output of 2 kW	280 – 420 V	310 V	Pass
System efficiency at 10 cm airgap and 0 cm offset	> 85%	91.69%	Pass
System efficiency at 15 cm airgap and 0 cm offset	> 85%	88.00%	Pass
System efficiency at 10 cm airgap and 10 cm offset	> 80%	89.77%	Pass
System efficiency at 15 cm airgap and 10 cm offset	> 80%	84.59%	Pass

6. PRACTICAL IMPLEMENTATION CONSIDERATIONS

While the 2-kW prototype successfully validates the coil design methodology, transitioning to a commercial product requires addressing further practical challenges, primarily related to electromagnetic interference (EMI) and thermal management. In a practical WPT system, managing EMI is critical for safety and regulatory compliance. To evaluate the effectiveness of shielding for the optimized coil, an FEA simulation was conducted. As shown in Figure 14(a), the unshielded coil exhibits significant magnetic field leakage, which could induce eddy currents in a vehicle's chassis. Figure 14(b) shows the result of adding a ferrite plate behind the coil to guide the flux and an aluminum plate to contain stray fields. The simulation confirms that this shielding strategy effectively reduces magnetic field leakage by 60%, ensuring the field is concentrated between the coils and minimizing potential interference.

Simultaneously, thermal management is necessary to prevent the coils from overheating, which can damage insulation and increase resistive losses. At the 2-kW power level and 85 kHz operating frequency, the use of Litz wire is a primary strategy to reduce AC resistance caused by skin and proximity effects, thereby minimizing heat generation. For a production system, a dedicated thermal analysis using FEA would be required to predict the temperature rise under continuous operation. Depending on the results, passive cooling through natural convection or an active cooling system might be necessary to maintain the coil temperature within safe operating limits.

The presented experimental setup utilizes a full-bridge inverter on the transmitter side and a full-wave rectifier on the receiver side. In this work, the output power was maintained at 2 kW by manually adjusting the input voltage source. In a commercial application, a closed-loop control system is essential for regulating power and maintaining high efficiency under varying load conditions and coil misalignments. Common control strategies include phase-shift control of the inverter legs or adjusting the switching frequency to maintain resonance and achieve zero voltage switching (ZVS), thereby minimizing switching losses in the power electronics devices.

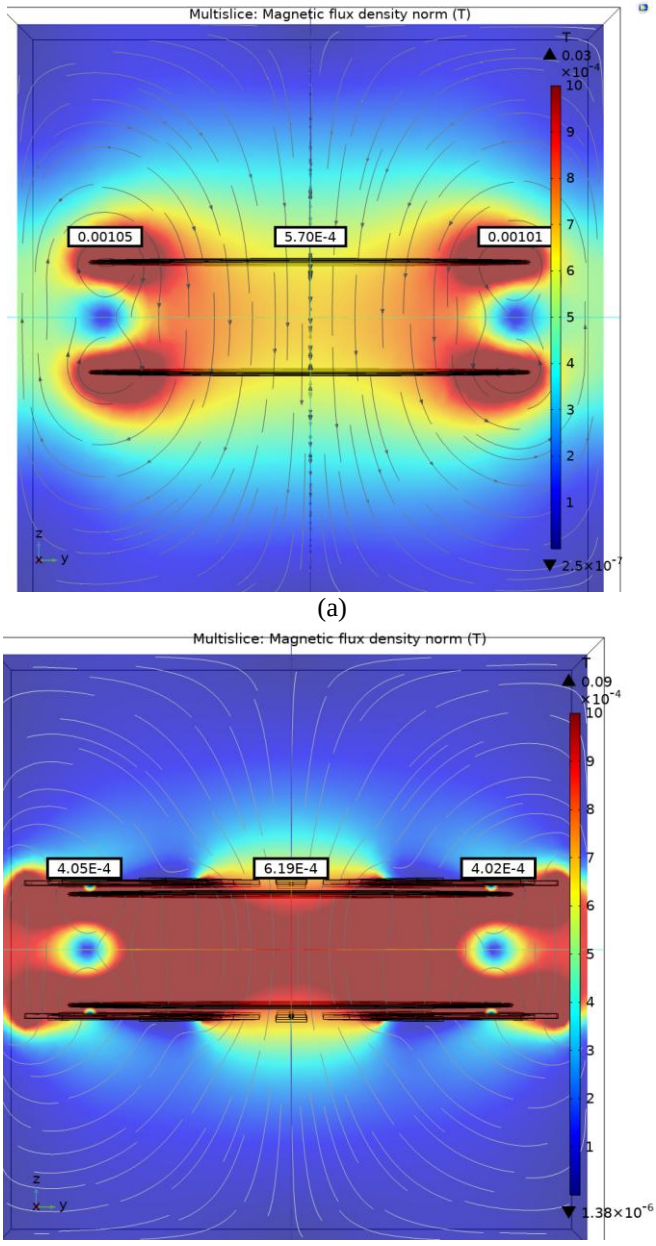

(a)

(b)

Figure 14. Finite element simulation: (a) without shielding and (b) with shielding

7. CONCLUSION

The design approach for the wireless EV charging system, aimed at meeting the performance requirements of the SAE J2954 standard, is presented in this paper. It focuses on the design of the coupled coil, as it has a significant impact on the overall system performance. The flowchart-based design technique is introduced to optimize key parameters of the flat spiral coil configuration, including the coil turn number, coil inner diameter, and coil outer diameter. The design process is governed by constraints, including a coil inductance of 200 μH, zero turn spacing, a copper wire diameter of 4 mm, and a maximum outer diameter of 700 mm. The results of the optimal coil design satisfy all constraints and comply with the wheeler condition. The FEA simulation using COMSOL software indicates that the magnetic coupling coefficient of the coupled coil is maximized when the optimal coil parameters, derived from the design process, are employed. The error between the fabricated and designed coil inductances is within 5%, confirming the validity of the wheeler condition. Four coil alignments, corresponding to the performance requirements of the SAE J2954 standard, are investigated, which are 10 cm air gap with 0 cm offset, 10 cm air gap with 10 cm offset, 15 cm air gap with 0 cm offset, and 15 cm air gap with 10 cm offset. The measured results of the magnetic coupling

coefficient, at different horizontal misalignments (offset) ranging from 0 to 10 cm, show good agreement with the FEA simulation results. The experimental results of the 2-kW prototype illustrate that system efficiency decreases with increasing air gap and/or horizontal misalignment between the coils, consistent with the relationship between magnetic coupling and coil offset. The measured system efficiency values exceed 85% and 80% for the 0 cm and 10 cm horizontal misalignment cases, respectively, meeting the required performance criteria. The test results of the four coil alignment cases indicate that the system performance complies with the requirements established in the SAE J2954 standard, thereby validating the proposed technique. This can be regarded as a guideline for developing high-performance wireless EV chargers that comply with the SAE J2954 standard. Future work will focus on integrating this optimized coil set into a complete system with a closed-loop controller to analyze dynamic response and load regulation. Furthermore, a comprehensive study on EMI shielding, thermal performance, and a comparative analysis with other coil topologies, such as DD and DSSq will be conducted to prepare the system for real-world deployment. These steps will further enhance the robustness of the proposed design for commercial EV charging applications.

FUNDING INFORMATION

This research project is supported by King Mongkut's University of Technology Thonburi (KMUTT), Thailand Science Research and Innovation (TSRI), and National Science, Research and Innovation Fund (NSRF), Fiscal year 2026 Grant number FRB690020/0164.

AUTHOR CONTRIBUTIONS STATEMENT

This journal uses the Contributor Roles Taxonomy (CRediT) to recognize individual author contributions, reduce authorship disputes, and facilitate collaboration.

Name of Author	C	M	So	Va	Fo	I	R	D	O	E	Vi	Su	P	Fu
Patcharapon Kaewnoen			✓	✓	✓	✓		✓	✓		✓			
Supapong Nutwong	✓	✓					✓			✓		✓	✓	
Nattapong Hatchavanich	✓	✓					✓			✓		✓		✓
Ekkachai Mujjalinvimut	✓	✓					✓			✓		✓		

C : **C**onceptualization
M : **M**ethodology
So : **So**ftware
Va : **Va**lidation
Fo : **Fo**rmal analysis
I : **I**nvestigation
R : **R**esources
D : **D**ata Curation
O : Writing - **O**riginal Draft
E : Writing - Review & **E**diting
Vi : **Vi**sualization
Su : **Su**pervision
P : **P**roject administration
Fu : **Fu**nding acquisition

CONFLICT OF INTEREST STATEMENT

Authors state no conflict of interest.

DATA AVAILABILITY

The data that support the findings of this study are available from the corresponding author, [SN], upon reasonable request.

REFERENCES

[1] International Energy Agency, "Global EV outlook 2023," *International Energy Agency*. IEA, 2023. [Online]. Available: https://www.iea.org/reports/global-ev-outlook-2023.
[2] M. Ehsani, K. V. Singh, H. O. Bansal, and R. T. Mehrjardi, "State of the art and trends in electric and hybrid electric vehicles," *Proceedings of the IEEE*, vol. 109, no. 6, pp. 967–984, Jun. 2021, doi: 10.1109/JPROC.2021.3072788.
[3] D. Ronanki and H. Karneddi, "Electric vehicle charging infrastructure: Review, cyber security considerations, potential impacts, countermeasures, and future trends," *IEEE Journal of Emerging and Selected Topics in Power Electronics*, vol. 12, no. 1, pp. 242–256, Feb. 2024, doi: 10.1109/JESTPE.2023.3336997.
[4] S. S. G. Acharige, M. E. Haque, M. T. Arif, N. Hosseinzadeh, K. N. Hasan, and A. M. T. Oo, "Review of electric vehicle charging technologies, standards, architectures, and converter configurations," *IEEE Access*, vol. 11, pp. 41218–41255, 2023, doi: 10.1109/ACCESS.2023.3267164.
[5] M. R. Khalid, I. A. Khan, S. Hameed, M. S. J. Asghar, and J. Ro, "A comprehensive review on structural topologies, power levels, energy storage systems, and standards for electric vehicle charging stations and their impacts on grid," *IEEE Access*, vol. 9, pp. 128069–128094, 2021, doi: 10.1109/ACCESS.2021.3112189.

[6] Z. Zhang, H. Pang, A. Georgiadis, and C. Cecati, "Wireless power transfer—An overview," *IEEE Transactions on Industrial Electronics*, vol. 66, no. 2, pp. 1044–1058, Feb. 2019, doi: 10.1109/TIE.2018.2835378.
[7] A. Alabsi *et al.*, "Wireless power transfer technologies, applications, and future trends: A review," *IEEE Transactions on Sustainable Computing*, vol. 10, no. 1, pp. 1–17, 2025, doi: 10.1109/TSUSC.2024.3380607.
[8] M. Rehman *et al.*, "A review of inductive power transfer: Emphasis on performance parameters, compensation topologies and coil design aspects," *IEEE Access*, vol. 11, pp. 144978–145010, 2023, doi: 10.1109/ACCESS.2023.3344041.
[9] A. Mahesh, B. Chokkalingam, and L. Mihet-Popa, "Inductive wireless power transfer charging for electric vehicles–A review," *IEEE Access*, vol. 9, pp. 137667–137713, 2021, doi: 10.1109/ACCESS.2021.3116678.
[10] Y. Komiyama *et al.*, "Analysis and design of high-frequency WPT system using load-independent inverter with robustness against load variations and coil misalignment," *IEEE Access*, vol. 12, pp. 23043–23056, 2024, doi: 10.1109/ACCESS.2024.3361029.
[11] S. Ghazizadeh, S. Mekhilef, M. Seyedmahmoudian, J. Chandran, and A. Stojcevski, "Performance evaluation of coil design in inductive power transfer for electric vehicles," *IEEE Access*, vol. 12, pp. 108201–108223, 2024, doi: 10.1109/ACCESS.2024.3439027.
[12] L. Yang *et al.*, "A high-efficiency integrated LCC/S WPT system with constant current output," *IEEE Journal of Emerging and Selected Topics in Power Electronics*, vol. 12, no. 1, pp. 341–354, Feb. 2024, doi: 10.1109/JESTPE.2023.3290214.
[13] V. Ramakrishnan *et al.*, "A comprehensive review on efficiency enhancement of wireless charging system for the electric vehicles applications," *IEEE Access*, vol. 12, pp. 46967–46994, 2024, doi: 10.1109/ACCESS.2024.3378303.
[14] Z. Dai, J. Wang, H. Zhou, and H. Huang, "A review on the recent development in the design and optimization of magnetic coupling mechanism of wireless power transmission," *IEEE Systems Journal*, vol. 14, no. 3, pp. 4368–4381, Sep. 2020, doi: 10.1109/JSYST.2020.3004201.
[15] V. Ramadoss, B. Chandrasekar, M. M. R. Ahmed, D. Savio A, N. Rajamanickam, and T. A. H. Alghamdi, "Research insights on recent power converter topologies and control strategies for wireless EV chargers: A comprehensive study," *IEEE Open Journal of Power Electronics*, vol. 5, pp. 1641–1658, 2024, doi: 10.1109/OJPEL.2024.3474707.
[16] B. Sim *et al.*, "A near field analytical model for EMI reduction and efficiency enhancement using an n th harmonic frequency shielding coil in a loosely coupled automotive WPT system," *IEEE Transactions on Electromagnetic Compatibility*, vol. 63, no. 3, pp. 935–946, Jun. 2021, doi: 10.1109/TEMC.2020.3039412.
[17] P. Deng, C. Tang, M. Sun, Z. Liu, H. Hu, and T. Lin, "EMI suppression method for LCC-S MC-WPT systems by parameter optimization," *IEEE Transactions on Power Electronics*, vol. 39, no. 9, pp. 11134–11147, Sep. 2024, doi: 10.1109/TPEL.2024.3414343.
[18] SAE Standard, "Wireless power transfer for light-duty plug-in/electric vehicles and alignment methodology," *Sae J2954*, p. J2954_202408, 2024, [Online]. Available: https://www.sae.org/standards/content/j2954_202408/.
[19] W. V. Wang, F. J. Lin, D. J. Thrimawithana, and G. Covic, "A modular multilevel converter based inductive power transfer system," in *2021 IEEE Energy Conversion Congress and Exposition (ECCE)*, Oct. 2021, pp. 5761–5766. doi: 10.1109/ECCE47101.2021.9595377.
[20] W. V. Wang and D. J. Thrimawithana, "A novel converter topology for a primary-side controlled wireless EV charger with a wide operation range," *IEEE Journal of Emerging and Selected Topics in Industrial Electronics*, vol. 1, no. 1, pp. 36–45, Jul. 2020, doi: 10.1109/JESTIE.2020.3003357.
[21] Rajanikant and V. Agarwal, "A novel misalignment tolerant DSSq receiver pad for wireless EV charging applications," in *2024 IEEE Energy Conversion Congress and Exposition (ECCE)*, Oct. 2024, pp. 1970–1975. doi: 10.1109/ECCE55643.2024.10861110.
[22] Y. Yao, S. Gao, J. Mai, X. Liu, X. Zhang, and D. Xu, "A novel misalignment tolerant magnetic coupler for electric vehicle wireless charging," *IEEE Journal of Emerging and Selected Topics in Industrial Electronics*, vol. 3, no. 2, pp. 219–229, Apr. 2022, doi: 10.1109/JESTIE.2021.3051550.
[23] C. Liu, X. Gao, and S. Cui, "A dual-layer receiver with low interlayer voltage stress and high power density for EVs wireless charging system," *IEEE Transactions on Industrial Electronics*, vol. 72, no. 4, pp. 3551–3561, Apr. 2025, doi: 10.1109/TIE.2024.3451140.
[24] E. Chaidee, A. Sangswang, S. Naetiladdanon, and S. Nutwong, "An inverter topology for multitransmitter wireless power transfer systems," *IEEE Access*, vol. 10, pp. 36592–36605, 2022, doi: 10.1109/ACCESS.2022.3162906.
[25] J. Cai, Y. Chen, A. David Cheok, Y. Yan, and X. Zhang, "Overview of coupling coil design for magnetic coupled resonance wireless charging system of electric vehicles," *IEEE Transactions on Transportation Electrification*, vol. 11, no. 4, pp. 8903–8918, Aug. 2025, doi: 10.1109/TTE.2025.3565803.
[26] M. Budhia, G. A. Covic, and J. T. Boys, "Design and optimization of circular magnetic structures for lumped inductive power transfer systems," *IEEE Transactions on Power Electronics*, vol. 26, no. 11, pp. 3096–3108, Nov. 2011, doi: 10.1109/TPEL.2011.2143730.
[27] B. H. Waters, B. J. Mahoney, G. Lee, and J. R. Smith, "Optimal coil size ratios for wireless power transfer applications," in *2014 IEEE International Symposium on Circuits and Systems (ISCAS)*, Jun. 2014, pp. 2045–2048. doi: 10.1109/ISCAS.2014.6865567.
[28] Y. Ben Fadhel, G. Bouattour, D. Bouchaala, N. Derbel, and O. Kanoun, "Model-based optimization of spiral coils for improving wireless power transfer," *Energies*, vol. 16, no. 19, p. 6886, Sep. 2023, doi: 10.3390/en16196886.
[29] M. Kim, M. Jeong, M. Cardone, and J. Choi, "Optimization of spiral coil design for WPT systems using machine learning," in *2023 IEEE Applied Power Electronics Conference and Exposition (APEC)*, Mar. 2023, pp. 822–828. doi: 10.1109/APEC43580.2023.10131149.
[30] M. Konghirun, S. Nutwong, A. Sangswang, and N. Hatchavanich, "Design of the transmitter coil used in wireless power transfer system based on genetic algorithm," *International Journal of Power Electronics and Drive Systems (IJPEDS)*, vol. 14, no. 4, p. 2307, Dec. 2023, doi: 10.11591/ijpeds.v14.i4.pp2307-2318.
[31] N. Prosen and J. Domajnko, "Optimization of a circular planar spiral wireless power transfer coil using a genetic algorithm," *Electronics*, vol. 13, no. 5, p. 978, Mar. 2024, doi: 10.3390/electronics13050978.
[32] S. S. Kalkute, D. S. Deokate, U. U. Jagtap, and D. S. Yeole, "Efficient coil design for 500W wireless power transfer for EV charging using Ansys Maxwell," in *2024 IEEE International Conference on Smart Power Control and Renewable Energy (ICSPCRE)*, Jul. 2024, pp. 1–4. doi: 10.1109/ICSPCRE62303.2024.10674994.

BIOGRAPHIES OF AUTHORS

Patcharapon Kaewnoen is a third-year undergraduate student in the Department of Electrical Engineering at King Mongkut's University of Technology Thonburi (KMUTT), Bangkok, Thailand. His interests span wireless power transfer, power electronics, IoT, and data-driven energy solutions. He has experience in embedded systems, machine learning applications for energy systems, and electrical system design, with proficiency in tools such as MATLAB/Simulink, LTspice, AutoCAD, and various programming languages, including Python and C. His work also extends to technological innovation and product development, particularly in energy and power electronics applications. He is passionate about integrating AI and smart energy systems to contribute to the advancement of sustainable and efficient technologies. He can be contacted at email: patcharapon.kaew@kmutt.ac.th.

Supapong Nutwong is a lecturer in the Electrical Engineering Department, Faculty of Engineering, King Mongkut's University of Technology Thonburi (KMUTT), Bangkok, Thailand, since 2020. He received the B.Eng. degree and M.Eng. degree in Electrical Engineering from the King Mongkut's University of Technology Thonburi in 2007 and 2011, respectively, and the D.Eng. degree in Electrical and Information Engineering Technology from the King Mongkut's University of Technology Thonburi in 2019. From 2013 to 2014, he was a Researcher at the Educational Support Unit, KMUTT. Since 2022, he has been an Assistant Professor with the Department of Electrical Engineering, KMUTT. His research interests include the field of power electronics, inductive power transfer (IPT) systems, capacitive power transfer (CPT) systems, wireless charging applications, and induction heating systems. He can be contacted at email: supapong.nut@kmutt.ac.th

Nattapong Hatchavanich is a lecturer in the Electrical Engineering Department, Faculty of Engineering, King Mongkut's University of Technology Thonburi (KMUTT), Bangkok, Thailand, since 2021. He received the B.Eng. degree in Electrical Engineering from the King Mongkut's University of Technology North Bangkok (KMUTNB) in 2012; received the M.Eng. degree in Electrical Engineering from the King Mongkut's University of Technology Thonburi in 2016; and the D.Eng. degree in Electrical and Information Engineering Technology from the King Mongkut's University of Technology Thonburi in 2020. His current research interests include the resonant inverter and control technique for wireless power transfer systems (WPT) and induction heating applications. He can be contacted at email: nattapong.hat@kmutt.ac.th.

Ekkachai Mujjalinvimut is a lecturer in the Electrical Engineering Department, Faculty of Engineering, King Mongkut's University of Technology Thonburi (KMUTT), Bangkok, Thailand, since 2016. He received the B.Eng. degree and M.Eng. degree in Electrical Engineering from the King Mongkut's University of Technology Thonburi in 2007 and 2009, respectively, and the D.Eng. degree in Electrical and Information Engineering Technology from the King Mongkut's University of Technology Thonburi in 2016. Since 2019, he has been an assistant professor with the Department of Electrical Engineering, KMUTT. His current research interests include switched-mode power supplies, applications of nonlinear control theory, and digital control. He can be contacted at email: ekkachai.muj@kmutt.ac.th.